J. Phys. D: Appl. Phys. **42** (2009) 105301 (5pp) doi:10.1088/0022-3727/42/10/105301

Flexible organic light-emitting diodes consisting of a platinum doped indium tin oxide anode

Ching-Ming Hsu, Chieh-Yang Huang, Hsyi-En Cheng and Wen-Tuan Wu

Department of Electro-Optical Engineering, Southern Taiwan University, 1 Nan-Tai Street, Yung-Kang City, Tainan County 710, Taiwan

E-mail: tedhsu@mail.stut.edu.tw

Received 31 December 2008, in final form 19 February 2009
Published 24 April 2009
Online at stacks.iop.org/JPhysD/42/105301

Abstract

This paper demonstrates that a flexible organic light-emitting diode (OLED) with a platinum (Pt)-doped indium tin oxide (ITO) anode could show superior electro-optical characteristics to those of a conventional device. The threshold voltage and turn-on voltage of an OLED device consisting of an aluminium/lithium fluoride/tris(8-hydroxyquinoline) aluminium/*N*,*N*′-bis-(1-naphthyl)-*N*,*N*′-diphenyl-1,1′-biphenyl-4,4′-diamine/Pt-doped ITO/ITO structure were reduced by 1.2 V and 0.8 V, respectively. Current efficiency was found improved for a driving voltage of less than 6.5 V as a result of the enhanced hole-injection rate, attributed mainly to the elevated surface work function and partly reduced surface roughness of ITO by the incorporated Pt atoms in the ITO matrix.

(Some figures in this article are in colour only in the electronic version)

1. Introduction

Organic light-emitting diodes (OLEDs) have been regarded as the best display device among the existing displays, owing to their superior opto-electrical characteristics and simple device architectures. Indeed, remarkable studies following the discovery of highly efficient OLED by Tang and VanSlyke in 1987 [1] have driven this display device to become a glass-based commercial product with outstanding performance. OLEDs have also received high prospects in applications for next generation high-quality flexible displays due to their relatively low process temperature. Research directed towards realizing the feasibility for OLEDs to be adopted on flexible substrates has been largely increasing [2–6]. The enhancement in device efficiency, lifetime and mechanical durability are being intensively studied.

One of the main topics of interest in enhancing device efficiency and lifetime is the interfacial treatment of indium tin oxide (ITO) that is commonly used as the anode material for OLED devices. For instance, surface treatments using UV ozone exposure [7, 8], gaseous plasma [9–12] and chemical liquid immersion [13–15] are able to raise surface work function of ITO film from its conventional value of 4.4 eV to a level around 4.7 eV, leading to the reduction of the barrier potential between the ITO anode and organic layers. Reduced operating voltage and enhanced device efficiency are generally obtained as a result of the surface treatments. Besides the work function, the interfacial morphology between the ITO anode and organic layers has been reported to play an important role in influencing device characteristics [16, 17]. Better contacts at the ITO/organic interfaces allow substantial delivery of hole carriers from the ITO anode to organic layers, and thus a high current efficiency is usually obtainable.

Adding a tin oxide layer between ITO and organic layers as reported by Parker and others [18–20] or doping high work function metals into the ITO matrix [21–24] has also been proposed in recent years for the same purpose. Particularly in the latter case the doped metals can simultaneously reduce the surface roughness of ITO film, which has been proved and generally admitted to be one of the key factors in improving device characteristics and lifetime [25–28]. For instance, OLED devices with the use of nickel(Ni)-doped ITO anodes have been demonstrated to have a reduced turn-on voltage by 2.3 V compared with conventional devices [23]. A systematic investigation of various doping metals that can raise the ITO work function and reduce surface roughness at a time is therefore an important issue to address.

In this paper we report on the preparation of platinum (Pt)-doped ITO films on flexible substrates using the

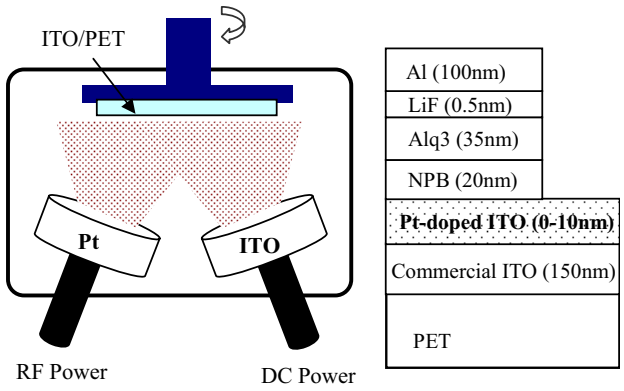

Figure 1. (Left) Schematics of the co-sputtering apparatus used for preparing Pt-doped ITO anode; (right) structure of bottom emission OLED device with a Pt-doped ITO anode.

co-sputtering approach. The effects of these films on the performance of OLED devices with a structure of aluminium(Al)/lithium fluoride (LiF)/tris(8-hydroxyquinoline) aluminium(Alq3)/*N*,*N*′-bis-(1-naphthyl)-*N*,*N*′-diphenyl-1,1′-biphenyl-4,4′-diamine(NPB)/Pt-doped ITO are investigated. The employment of Pt was based on the fact that it has a higher nominal work function (5.4 eV) than Ni (5.0 eV). Therefore, it is expected that OLED devices with a Pt-doped ITO anode should show better characteristics.

2. Experiments

OLED bottom emission devices with an Al(100 nm)/LiF(0.5 nm)/Alq3(35 nm)/NPB(20 nm)/Pt-doped ITO structure, as schematically illustrated in figure 1, were fabricated on commercial ITO(150 nm)/Arton substrates. The preparation of the devices started with the deposition of a Pt-doped ITO film using a co-sputtering approach (figure 1) to a thickness of 0, 2, 6 and 10 nm. The Pt target was sputtered at an rf power of 10 W and the ITO target at a dc power of 80 W, yielding a Pt concentration of 1.2 at% measured by an Auger electron spectrometer. The substrates were heated to a temperature of 100 °C for deposition and the process pressure was kept at 3 mTorr. A metallic shadow mask was attached to the substrate to define the pattern of the ITO anode.

These substrates were then loaded into a cluster-type deposition system with which consecutive processes could be conducted without breaking the vacuum. Surface treatment with oxygen plasma was first conducted before the substrate was transferred to a thermal evaporator to coat the NPB and Alq3 layers. The NPB serves as the hole-transport layer and the Alq3 as the emissive and electron-transport layer. The deposition rate for both the NPB and Alq3 layers was kept at 0.5 nm s^{-1} in an ambient of 2×10^{-6} Torr and the flexible Arton substrate was not heated during deposition. The depositions of the LiF and Al layers were followed in sequence by electron-beam evaporation in another process chamber to form the cathode electrode at room temperature. The complete devices were then immediately characterized after being unloaded from the process system.

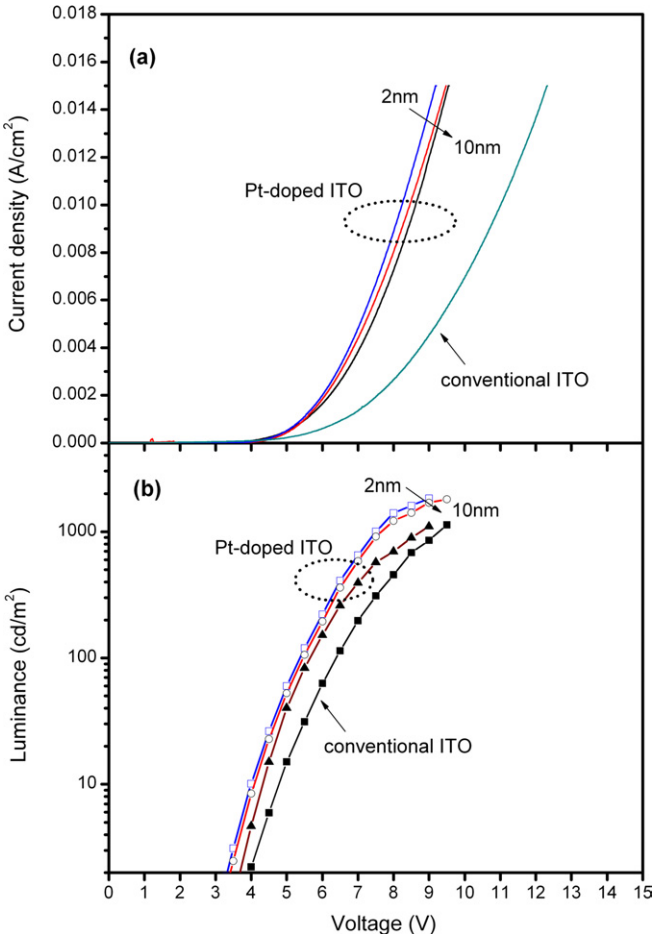

Figure 2. (*a*) *J*–*V* (*b*) *L*–*V* characteristics of OLED devices with and without a Pt-doped ITO anode.

Table 1. The comparison of threshold voltage and turn-on voltage of OLED devices with various thicknesses of Pt-doped ITO anode. Also presented are the optical transmittance and surface roughness of the ITO anodes.

	Thickness of Pt-doped ITO			
	0 nm	2 nm	6 nm	10 nm
V_T (V) at 1 mA cm^{-2}	6.60	5.44	5.50	5.54
V_{ON} (V) at 10 cd m^{-2}	4.78	4.0	4.07	4.3
Optical transmittance at 510 nm	87.0	85.3	84.2	82.4
ITO surface roughness (R_a, nm)	1.02	0.52	0.59	0.63

3. Results and discussions

Figures 2(*a*) and (*b*) plot the current density–voltage (*J*–*V*) and the luminance–voltage (*L*–*V*) characteristics of these OLED devices, respectively. The devices consisting of a Pt-doped anode apparently exhibit improved *J*–*V* and *L*–*V* characteristics with the curves shifting to the lower end of voltage. The corresponding threshold voltage (determined at 1 mA cm^{-2}) and turn-on voltage (determined at 10 cd m^{-2}) are listed in table 1. Compared with the conventional device, a reduction in the threshold voltage by ∼1.2 V and the turn-on voltage by ∼0.8 V is observed for the device with a 2 nm Pt-doped ITO anode. Measurement with a Riken Keiki AC-2 photoelectron spectroscope reveals that the work function is

4.95 and 4.76 eV for the Pt-doped ITO and the commercial ITO, respectively. Hence it is evidently presumed that the doping of Pt atoms elevates the ITO work function, leading to the improved J–V and L–V characteristics of the Pt-doped devices.

Figure 2 also reveals that OLED devices with a 2 and a 6 nm Pt-doped ITO anode display slightly better J–V and L–V characteristics than the one with a 10 nm anode. When driven at voltages higher than the threshold voltage, the 2 nm Pt-doped device was found to have an external luminance intensity at least 40% higher than the 10 nm device. Since the thickness and the surface topography are basically the main differences among these Pt-doped ITO anodes, the discrepancy in the external luminance intensity should be caused by (1) the optical loss across the Pt-doped ITO layer and (2) the ITO/NPB interfacial morphology (state of contacts). We examined the optical transmittance (measured at 510 nm of the device spectral peak) for various Pt-doped ITO films as shown in table 1, from which an optical loss of 3.1% can be observed as the thickness of the Pt-doped ITO film increases from 2 to 10 nm. This suggests that the optical loss is a minor factor in the deteriorated L–V characteristic as the thickness of the Pt-doped ITO film is increased. The main factor in device degradation of this kind is then considered to be the interfacial morphology. One can see from table 1 that the conventional ITO film has the highest surface roughness (determined by atomic force microscopy), whereas the 10 nm Pt-doped ITO film is the worst among the doped films. It is well known that a rough ITO surface generally leads to the deterioration of the light-emitting process by the local Joule-heat mechanism [29, 30]. The rough ITO surface also results in a poor contact between ITO and organics, rendering a worse hole-injection probability at the interfaces [31]. In our case, better contacts at the ITO/NPB interfaces allow more carriers to inject into organic layers and help to yield a higher recombination rate (R) according to the well-known relationship $R = \beta np$ (n is the electron concentration, p the hole concentration and β the recombination probability). A light-emitting device having a high carrier recombination can normally generate a high light output. Hence, it is reasonable to deduce that the improved ITO surface roughness due to the co-sputtering of Pt atoms also contributes in enhancing the electro-optical characteristics of an OLED device. This phenomenon was also observed for devices with a Ni-doped ITO anode as reported elsewhere [27]. However, the mechanism by which the addition of minority metallic atoms improves the ITO film surface roughness during ITO sputtering is not clear yet. It also has to be noted that the improved surface roughness overall plays a minor role in the improved J–V and L–V characteristics compared with the effect from the elevation in the ITO surface work function.

Figure 3 demonstrates the current efficiency as a function of driving voltage for devices with various thicknesses of Pt-doped ITO anode. The current efficiency is defined as the luminance divided by the current density ($\eta_c = L/J$). From the figure one can see that devices with a Pt-doped ITO anode possess higher current efficiency as the driving voltage is less than 6.5 V. As derived from the J–V characteristics, at 6.5 V the current density for the 2 nm Pt-doped device (3.2 mA cm^{-2})

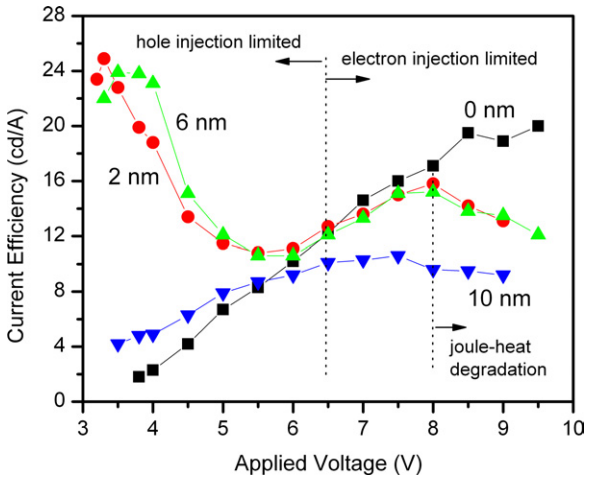

Figure 3. Current efficiency as a function of driving voltage for OLED devices with and without a Pt-doped ITO anode.

is 3.5 times that of the conventional device (0.94 mA cm^{-2}), indicating the Pt-doped device received many more holes from the anode. Therefore the Pt-doped devices presumably not only have a higher hole-injection rate (due to the increased work function and partly the reduced surface roughness) but also a higher hole–electron recombination rate for a driving voltage of less than 6.5 V. A particular phenomenon can be seen for voltages below 4 V where the current efficiency of 2 and 6 nm Pt-doped devices is relatively high. This is due to their extremely low current densities (10^{-7}–10^{-4} A cm^{-2}) and detectable light output in the sub-threshold region. Besides, the current increases more rapidly than the emitted light does in this region, bringing about a drop in current efficiency with the increasing voltage. This regional high current efficiency however provides little physical meaning for the Pt-doped devices since it occurs in the range below the defined turn-on voltage.

When the driving voltage is greater than 6.5 V, the Pt-doped OLED device appears to have a lower current efficiency than the conventional device. This is perhaps not caused by the degradation of the light-emitting process of the Pt-doped OLED device, because the current efficiency still increases with increasing voltage in this region. The degradation process should merely become effective for driving voltages greater than 8 V where the current efficiency of the Pt-doped device starts to fall. The relative low current efficiency of Pt-doped devices for driving voltages between 6.5 and 8 V is then considered to be due to the unbalanced hole–electron recombination. That is, there are excessive holes without recombining with electrons in the emissive layer, and these redundant holes do not help to generate high optical output but substantially contribute to the total current density. Theoretically the external optical output is proportional to the internal quantum efficiency which is directly proportional to the carrier recombination rate, R. And according to the relationship $R = \beta np$, as discussed previously, the current efficiency can then be expressed as $\eta_c = L/J \propto np/(n + p)$. When the hole concentration is much greater than the electron concentration ($p \gg n$), the current efficiency becomes proportional to the electron concentration ($\eta_c \propto n$). This

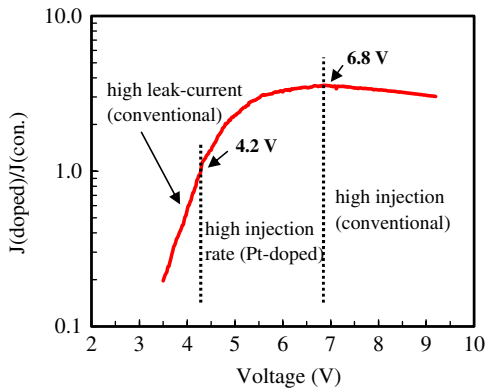

Figure 4. Dependence of current density ratio J(doped)/J(con.) on driving voltage. A 2 nm Pt-doped OLED device was used in this case.

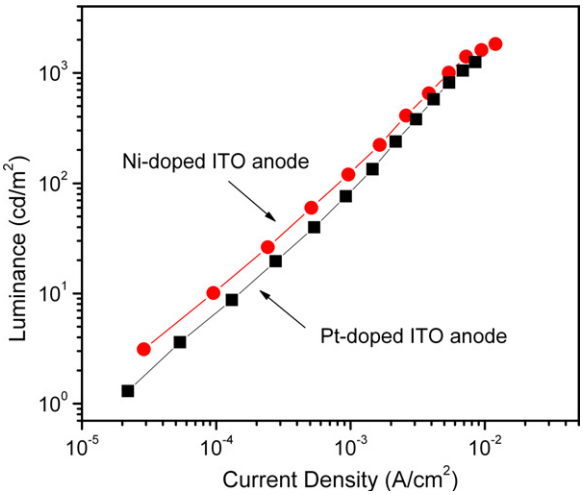

Figure 5. Luminance–current density (L-J) characteristics of OLED devices with a Ni(2 nm) and a Pt(10 nm) doped ITO anode.

implies that the current efficiency is dominated mainly by the electron concentration when there are considerably excessive holes in the emissive layer. Hence, although the use of a Pt-doped ITO anode can largely increase the hole-injection of an OLED device, the current efficiency will be limited by the electron injection at high driving voltages (>6.5 V in this case). To further extend the high current efficiency to a higher voltage end, one should then consider balancing the hole and electron concentrations by lowering the interfacial potential barrier at the cathode side. This agrees with the work done by Li *et al* [32] in which balanced hole and electron injections are reported to lead to a more efficient Alq3-based OLED devices.

Regarding the drop in current efficiency for voltages greater than 8 V, the Joule-heat caused degradation process is considered to play an important role. One can observe from the L–V characteristics of Pt-doped OLEDs that the luminance starts to saturate at 8 V, while from the J–V characteristics the current density still increases rapidly. This means the degradation of the light-emitting process becomes more serious at high current flows. It has been proved that the degradation processes such as the intrinsic degradation and the development of dark spots are generally more prominent at high temperatures [33, 34]. The Pt-doped OLED devices operated at high current flows (>8 V) should experience higher temperatures and thus accelerated Joule-heat degradation.

We examined the current density ratio of the 2 nm Pt-doped device to the conventional device, J(doped)/J(con.), as a function of the driving voltage, as shown in figure 4. It can be seen that the current density ratio largely increases with driving voltage up to around 6.8 V and then starts to drop afterwards at a moderate rate. Below 4.2 V, the current density ratio is less than 1, showing that the conventional device has a higher current density in the sub-threshold region. This is believed to be due to the high leakage current of the conventional device in this region. Above 4.2 V, the current density ratio is greater than 1, and the fact that the J(doped)/J(con.) increases with driving voltage indicates that hole carriers are injected into the NPB layer more rapidly from the Pt-doped ITO anode than from the conventional ITO. The reduced potential barrier at the ITO/NBP interfaces by the Pt-doped anode should again be the main cause. The current density ratio remains increasing until the driving voltage reaches 6.8 V at which the maximum J(doped)/J(con.) is 3.6. The corresponding current density is J(doped) = 4.14 mA cm^{-2} and J(con.) = 1.17 mA cm^{-2}. It is interesting that this voltage is close to the defined threshold voltage of the conventional device (6.6 V at 1 mA cm^{-2}) and to the point (V = 6.5 V) where the current efficiency of the Pt-doped device becomes less than the conventional device as depicted earlier. The coincidence implies that (1) the drop in J(doped)/J(con.) after 6.8 V is attributed to the rapid increase of carriers in the conventional device, (2) Pt-doped devices will always have a lower current efficiency than the conventional device provided the device is operated in the region beyond the threshold voltage of the conventional device.

Therefore as far as the current efficiency is concerned, the operational voltage for Pt-doped devices between 5.4 V (the threshold voltage of the 2 nm Pt-doped device) and 6.5 V (the current efficiency turning point) is suggested from the discussions above. This range is believed not to be sufficiently wide for operating an OLED device, and so further enhancement in the current efficiency is necessary. It is however not realistic to elevate the surface work function of ITO by introducing more Pt atoms in the ITO matrix because a slight increase in the Pt doping level will result in a large decrease in optical transmittance. We fabricated a Pt(30 W)-doped ITO to yield a surface work function of 5.02 eV, but its optical transmittance dropped to the level of 64%. This is not how a TCO film should appear. Instead, optimizing device stacked structures or raising the electron-injection rate from the cathode, as discussed earlier, are considered to be a more pertinent way to promote the hole–electron recombination rate and so forth the device efficiency in this Pt-doped ITO scheme.

Moreover contrary to the prior expectation, OLED devices with a Pt-doped ITO anode were found not necessary to show much better characteristics compared with a Ni-doped device. We fabricated another set of OLEDs with a Ni(10 nm, 1.8 at%) and a Pt(2 nm, 1.2 at%) doped ITO anode. The 10 nm Ni-doped film was used because it has an optical transmittance (~86.2%) close to that of the 2 nm Pt-doped film (~85.3%). Figure 5 compares the luminance–current density (L–J) characteristics

of these two devices. It clearly shows the Ni-doped OLED exhibits a slightly better J–V characteristic than the Pt-doped OLED. Results from Fourier transform infrared spectrometry suggest that Pt should appear in the ITO matrix mostly in the form of PtO_x. This explains why the Pt-doped ITO work function (∼5.0 eV) is actually much lower than the elemental platinum (5.4 eV). On the contrary, Ni-doped ITO film containing NiO_x phases in the matrix can exhibit a higher surface work function (>5.2 eV) than the nominal work function of Ni (5.1 eV) [27]. From this observation, it can be said that the work function of metal oxide rather than the metal itself is the dominating factor in elevating the level of the surface work function of a metal-doped ITO.

4. Conclusions

In summary, this work demonstrates that flexible OLED devices with a Pt-doped ITO anode could display better J–V and L–V characteristics than conventional devices, with a reduced threshold voltage of 1.2 V and turn-on voltage of 0.8 V. The improved device performance is attributed mainly to the elevated surface work function of ITO by the incorporated Pt atoms in the ITO matrix. Reduced ITO surface roughness due to the co-sputtering of Pt atoms is proved to be another factor that can result in the improved device characteristics. Pt-doped devices were found to have higher current efficiency for driving voltages of less than 6.5 V because of their enhanced hole-injection rates. At higher voltages, the current efficiency is limited by the cathode current and/or Joule-heat caused degradation. To promote further device efficiency, optimizing organic stacked structures and raising the electron-injection rate are suggested in this Pt-doped ITO scheme.

Acknowledgments

The authors would like to thank the National Science Council of Taiwan for financially supporting this work under Contract No NSC-95-2221-E-218-047. Special thanks also go to Professor T Mori of Nagoya University for the measurement of the surface work function of ITO.

References

[1] Tang C W and VanSlyke S A 1987 *Appl. Phys. Lett.* **51** 913
[2] Krasnova A N 2002 *Appl. Phys. Lett.* **80** 3853
[3] Lee L H and Jin C S 2002 *Mater. Lett.* **53** 227
[4] Hirotake K, Takayuki T and Yutaka O 2003 *Thin Solid Films* **438** 334
[5] Chwang A B *et al* 2003 *Appl. Phys. Lett.* **83** 413
[6] Lee S N, Hsu S F, Hwang S W and Chen C H 2004 *Curr. Appl. Phys.* **4** 651
[7] VanSlyke S A, Chen C H and Tang C W 1996 *Appl. Phys. Lett.* **69** 2160
[8] Hung L S, Tang C W and Mason M G 1997 *Appl. Phys. Lett.* **70** 152
[9] Wu C C, Wu C I, Sturm J C and Kahn A 1997 *Appl. Phys. Lett.* **70** 1348
[10] Lee C T, Yu Q X, Tang B T and Lee H Y 2001 *Thin Solid Films* **386** 105
[11] Lu H T and Yojoyama M 2004 *J. Cryst. Growth* **260** 186
[12] Hunag Z H, Zeng X T, Sun X Y, Kang E T, Fuh Y H and Lu L 2008 *Org. Electron.* **9** 51
[13] Sun X H, Cheng L F, Liu M W, Liao L S, Wong N B, Lee C S and Lee S T 2003 *Chem. Phys. Lett.* **370** 425
[14] Li F, Tang H, Shinar J, Resto O and Weisz S Z 1997 *Appl. Phys. Lett.* **70** 2741
[15] Osada T, Kugler T, Broms P and Salaneck W R 1998 *Synth. Met.* **96** 77
[16] Furukawa K, Terasaka Y, Ueda H and Matsumura M 1997 *Synth. Met.* **91** 99
[17] Andersson A, Johansson N, Broms P, Yu N, Lupo D and Salaneck R 1998 *Adv. Mater.* **10** 859
[18] Parker I D 1994 *J. Appl. Phys.* **75** 1656
[19] Blom P, Jong M and Vleggaar J 1996 *Appl. Phys. Lett.* **68** 3308
[20] Chan I M, Hsu T Y and Hong C 2002 *Appl. Phys. Lett.* **81** 1899
[21] Freeman A J, Poeppelemier K R, Mason T D, Chang R P and Marks T J 2000 *MRS Bull.* **25** 45
[22] Marks T J, Veinot J G, Cui J, Yan H, Wang A, Edleman N L, Ni J, Hunag Q, Lee P and Armstrong N R 2002 *Synth. Met.* **127** 29
[23] Hsu C M and Wu W T 2004 *Appl. Phys. Lett.* **85** 840
[24] Hsu C M, Tsai C L and Wu W T 2006 *Appl. Phys. Lett.* **88** 083515
[25] Park N G, Kwak M Y, Kim B O, Kwon O K, Kim Y K, You B, Kim T W and Kim Y S 2002 *Japan. J. Appl. Phys. Part 1* **41** 1523
[26] Hunag Z H, Zeng Z T, Kang E T, Fuh Y H, Lu L and Sun X Y 2006 *Electrochem. Solid State Lett.* **9** H39–42
[27] Hsu C M, Lee J W, Meen T H and Wu W T 2005 *Thin Solid Films* **474** 19
[28] Hsu C M, Wu W T and Lee H H 2008 *Displays* **29** 268
[29] Ishii M and Taga Y 2002 *Appl. Phys. Lett.* **80** 3430
[30] Lin K K, Chua S J and Wang W 2002 *Thin Solid Films* **417** 36
[31] Chen S F and Wang C W 2004 *Appl. Phys. Lett.* **85** 765
[32] Li W, Jones R A, Allen S C, Heikenfeld J C and Steckl A J 2006 *J. Display. Technol.* **2** 143
[33] Anjos P N M, Aziz H, Hu N X and Popovic Z D 2002 *Org. Electron.* **3** 9
[34] D'Andrade B W, Esler J and Brown J J 2006 *Synth. Met.* **156** 405